ADVANCED MATERIALS INTERFACES
www.advmatinterfaces.de

Spontaneous Assembly of Extremely Long, Horizontally-Aligned, Conductive Gold Micro-Wires in a Langmuir Monolayer Template

*Hao Jiang, T. P. Vinod, and Raz Jelinek**

"Bottom-up" technologies are based upon the premise that organized systems – from the nano-scale up to the macro-scale – can be assembled spontaneously from basic building blocks in solution. We demonstrate a simple strategy for the generation of extremely long (up to several centimeters), horizontally-aligned gold micro-wires, produced through a surfactant monolayer template deposited from gold thiocyanate [$Au(SCN)_4^-$] aqueous solution. Specifically, we show that the surfactant, octyl-maleimide (OM), spontaneously forms oriented micro-wires at the air/water interface, which constitute a template for deposition of metallic gold through binding and crystallization of the soluble gold complex. The Au micro-wires can be subsequently transferred onto solid substrates, and following plasma treatment and gold enhancement exhibit excellent conductivity even at electrode spacings of several centimeters. Importantly, the micro-wire alignment determines the direction of electrical current, demonstrating that long-range ordering of the micro-wires can be accomplished, significantly affecting the physical properties of the system. The new approach is simple, robust, and can be readily exploited for bottom-up fabrication of micro-wire assemblies and transparent conductive electrodes.

1. Introduction

Fabrication of nano- and micro-scale conductive wires that would further exhibit long-range organization is a highly sought albeit challenging goal in optoelectronic, photovoltaic, and nano-photonics research and development.[1–4] While most currently fabricated micro- and nano-electronic devices are produced via "top-down" lithography methods,[5–7] "bottom-up" approaches have emerged as promising alternatives for generation of organized nanostructures and electronic components.[8–10] Bottom-up techniques generally rely upon molecular self-assembly phenomena to produce defined structures that could be practically utilized.[11–13]

Many studies have focused on gold nanostructures as a versatile and powerful means for bottom-up synthesis schemes. The propensity of Au ions to self-assemble and undergo rapid reduction into colloids and NPs, however, poses distinct barriers for utilizing conventional gold chemistry for creating structurally-defined, organized wire structures and thin films. Patterned Au structures have been produced through chemical derivation of gold colloids surfaces[14] and/or the substrate employed for surface deposition,[15–17] or through the aid of physical templates.[18–22] These approaches exhibit shortcomings, both conceptually as well as technically. Specifically, Au NP synthesis and surface derivatization are often multi-step procedures and introduce certain variability in term of product uniformity. In addition, in many cases chemical treatment of NP-based films is further required after surface deposition of the NPs, presenting additional experimental parameters to modify and optimize. Furthermore, on a fundamental basis, the rapid reduction of ionic gold into metal NPs severely restricts the possibility to control the structural features and spatial, long-range organization of the metal assemblies.

We present a simple strategy for fabricating extremely long (up to several centimeters), horizontally-aligned, conductive gold micro-wires, produced through deposition of a surfactant monolayer upon gold thiocyanate [$Au(SCN)_4^-$] aqueous solution. We have recently demonstrated that $Au(SCN)_4^-$ self-assembles into conductive Au^0 nanostructures through single-step crystallization/reduction process which do not require addition of reducing agents.[23–25] Here we show that a surfactant, octyl-melamine (OM), adopts elongated and aligned micro-wire morphology when isothermally compressed at the air/water interface. Furthermore, the OM assemblies constitute a template for gold deposition through electrostatic attraction between the primary amine residues of the surfactant and soluble $Au(SCN)_4^-$, accompanied by spontaneous crystallization and reduction of gold by the thiocyanate moieties, without addition of reducing agents. In particular, previous studies have demonstrated that immobilization of the gold complex onto amine-displaying surfaces leads to crystalline organization that is largely promoted through aurophilic interactions among Au^I species. Reduction leading to metallic gold formation was found to occur concurrently with the crystallization process, overall resulting in surface-anchored Au^0 nanostructure

Dr. H. Jiang, Dr. T. P. Vinod, Prof. R. Jelinek
Department of Chemistry and Ilse Katz Institute for Nanotechnology
Ben Gurion University of the Negev
Beer Sheva 84105, Israel
E-mail: razj@bgu.ac.il

DOI: 10.1002/admi.201400187

formation; plasma treatment was further shown to complete the transformation of Au ions into the metallic species.[23]

The aligned gold micro-wires could be transferred from the air/water interface onto solid substrates. Following plasma treatment and gold enhancement the micro-wire films exhibited high optical transparency and excellent conductivity even at electrode spacings of several centimeters. Importantly, the alignment of the gold micro-wires effectively determined the direction of electrical current, demonstrating that macro-scale organization which affects the physical properties of the system could be accomplished.

2. Results and Discussion

Formation of conductive gold micro-wires was carried out through a simple "template-directed" synthesis scheme (**Figure 1**). Specifically, a Langmuir monolayer of the OM surfactant was deposited upon water subphase containing soluble $Au(SCN)_4^-$ (at a concentration of 10^{-5} M) (Figure 1A). Incubation gave rise to deposition of metallic gold upon the OM monolayer through a recently-reported process in which $Au(SCN)_4^-$ binds through electrostatic attraction to the OM amino residues, followed by crystallization and thiocyanate-induced reduction.[23] Remarkably, subsequent isothermal compression of the monolayer resulted in formation of aligned OM/gold micro-wires (Figure 1B). The micro-wires could be transferred from the water interface onto solid supports by the Langmuir-Schaffer method (horizontal transfer), and following plasma treatment (to remove the organic residues)[26] and gold enhancement[19,27] transparent and highly conductive films comprising the gold micro-wires are produced (Figure 1C).

Figure 2 and **3** present in situ and ex situ characterization of the micro-wires. Figure 2 shows a surface-pressure/area isotherm and corresponding Brewster angle microscopy (BAM) images of the OM monolayer deposited upon the $Au(SCN)_4^-$ subphase. The BAM images in Figure 2 demonstrate the formation of aligned, elongated micro-wires upon compression of

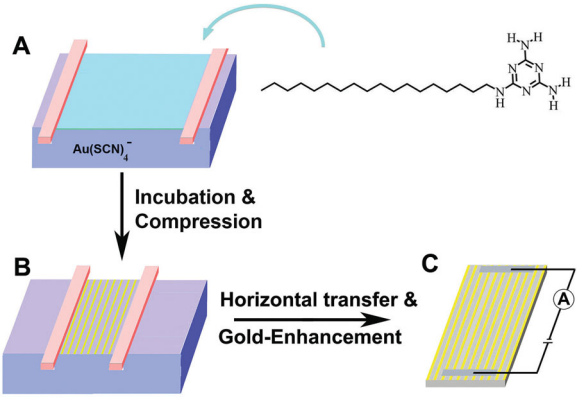

Figure 1. Experimental scheme (not in scale). (A) OM molecules are spread over aqueous subphase containing $Au(SCN)_4^-$. (B) After incubation, the monolayer is isothermally compressed resulting in the formation of aligned OM/gold micro-wires. (C) The micro-wires are transferred onto a solid substrate; plasma treatment and gold enhancement produce highly conductive, transparent gold micro-wire films.

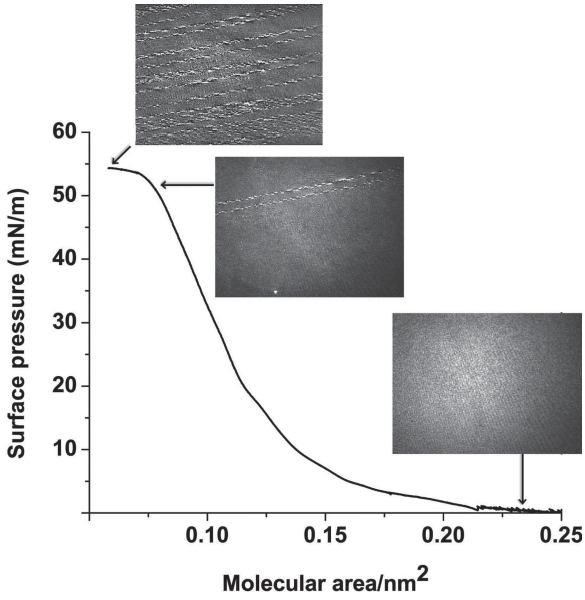

Figure 2. Micro-wire formation at the air/water interface. Surface-pressure/area isotherm of OM monolayer compressed upon a water subphase containing soluble $Au(SCN)_4^-$; BAM images above the isotherm were recorded at the surface pressures indicated by the arrows.

the monolayer. In a low surface pressure, the OM monolayer appeared uniform, covering the entire surface area (Figure 2, right image). However intense reflective strips corresponding to condensed Au/OM micro-wires appear when the surface pressure was increased approximately to 50 mN m^{-1} (Figure 2, middle image). The microwires became more abundant, while still aligned, upon further increase of the surface pressure (Figure 2, top left image).

Aligned micro-wire organization was observed also upon compression of OM on pure aqueous phase (not containing the gold thiocyanate complex, Figure S1) indicating that the micro-wire assembly was adopted by the OM alone, which consequently served as a template for gold deposition. The formation of micro-wire structures within the OM monolayer is likely ascribed to hydrogen-bonding and π–π stacking between adjacent melamine moieties.[28] Indeed, such interactions have been shown to have prominent roles in promoting organized surfactant structures in Langmuir monolayers.[29] Additional experiments corroborate the proposed contribution of hydrogen bonding to micro-wire formation. For example, changing the acidity of the aqueous subphase (from pH of 6.5 to 4) blocked formation of the micro-wires (Figure S2), presumably through disrupting the extent of hydrogen bond formation within the monolayer. After incubation and compression, the monolayer containing the aligned micro-wires was transferred by the Langmuir-Schaefer (LS) method (i.e., horizontal transfer) onto a hydrophobic solid substrate (silane-treated glass or silicon wafer). The glass-supported films were then subjected to brief plasma treatment to remove the organic (OM) template,[26] and gold enhancement procedure designed to augment the gold micro-wire features.[19,27] The enhancement process essentially utilized the micro-wires as a "scaffold catalyst" for docking additional gold layers.

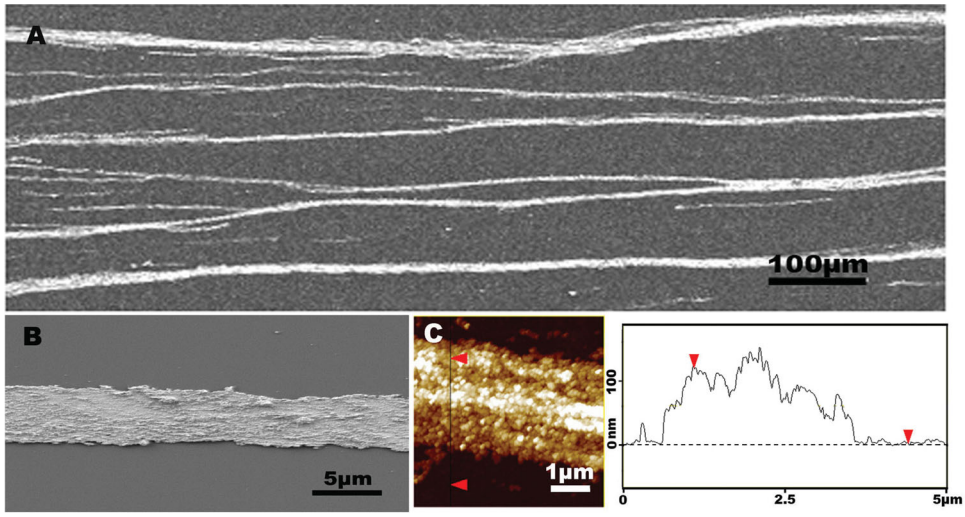

Figure 3. Microscopy characterization of the aligned gold micro-wires. (A) SEM image of a film region depicting the gold micro-wires following plasma treatment and gold enhancement; (B) SEM image of a small region of the micro-wire showing a continuous, dense gold coverage; (C) AFM image (left) and height profile of a region within a single micro-wire.

Figure 3 presents microscopy characterization of the micro-wire assemblies on silicon wafer after plasma treatment and gold enhancement. The scanning electron microscopy (SEM) image of a representative film region in Figure 3A highlights the formation of extremely long, macroscopically-aligned wires. The micro-wires appeared continuous up to lengths of several centimeters – essentially determined by the overall width of the Langmuir trough employed in the experiments. It should be noted that SEM measurements indicate that the aligned micro-wire organization was preserved through both plasma and gold enhancement processes (**Figure 4**). The SEM image (Figure 3B) and atomic force microscopy (AFM) results (Figure 3C) of a magnified view within a gold micro-wire reveal dense gold coating and indicate that the micro-wires exhibit widths of few microns and heights in the range of 100–300 nm.

Experimental data designed to examine the effect of isothermal compression and post-transfer treatment of the monolayers upon micro-wire organization is presented in Figure 4. Specifically, the SEM images in Figure 4 indicate that high surface pressure of the Langmuir monolayer did not adversely affect microwire morphology, but rather resulted in greater abundance and "crowdedness" of the transferred wires (Figure 4A). Similarly, micro-wire organization and integrity were retained following plasma treatment (Figure 4B) and gold enhancement (Figure 4C).

Spectroscopy analyses confirm that the micro-wires comprised of metallic gold (**Figure 5**). Specifically, the x-ray photoelectron spectroscopy (XPS, Figure 5A) spectrum feature the Au^0 4f peaks, while the powder x-ray diffraction (XRD, Figure 5B) spectrum highlights lattice planes of crystalline Au. Together, the XPS and XRD data in Figure 5 affirm that Au^0 was the predominant species in the micro-wires, both after transfer from the air/water interface onto the solid substrate (Figure 5A), as well as following plasma treatment and gold enhancement (Figure 5B). The spectroscopic data in Figure 5 – indicating Au^0 formation – are consistent with the gold deposition mechanism outlined above, according to which electrostatic attraction induced binding between the amine moieties of OM (which are positively-charged in the pH conditions employed) and the negatively-charged $Au(SCN)_4^-$, followed by spontaneous crystallization/reduction of the Au ions by the thiocyanate ligands.[23] Control experiments corroborated the proposed mechanism. No organized Au structures were formed, for example, upon (or within) the water subphase when OM monolayers were not present. Also, no gold micro-wires were assembled when the ionic strength of the subphase was increased (for example using a subphase containing 0.5 M KCl, Figure S3) – this inhibition effect is ascribed to electrostatic shielding of the OM monolayer by the positive potassium ions in the aqueous solution.[23]

The physical properties and potential applicability of glass-supported aligned gold micro-wire films in electro-optical devices were further examined (**Figure 6**). Figure 6 demonstrates excellent transparency and conductivity profiles of the aligned gold micro-wire films. Figure 6A shows close to 100% light transmittance in the visible spectrum range and well into the infrared (IR) region of the electromagnetic radiation. It should be noted that the transparency was dependent upon

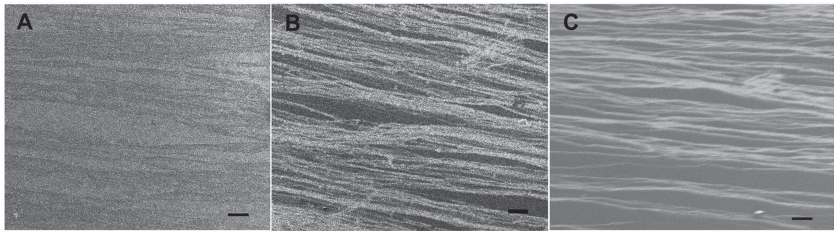

Figure 4. Effects of plasma treatment and gold enhancement upon Au micro-wires. SEM images depicting Au micro-wires transferred at a high surface pressure (55 mN/m) onto the hydrophobic substrate (A). The Au micro-wires after plasma treatment (B), and after gold enhancement (C). Scale bar: 100 μm.

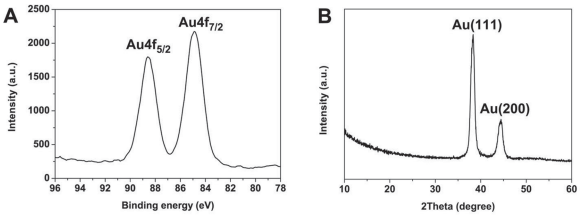

Figure 5. Spectroscopic confirmation that the micro-wires comprise of metallic Au. (A) x-ray photoelectron spectroscopy (XPS) spectrum of micro-wires transferred from the air/water interface onto solid substrate. (B) x-ray diffraction (XRD) pattern of the micro-wires after gold enhancement.

the abundance of micro-wires on the surface, however several measurements (employing different OM monolayer concentrations and surface pressures in which monolayers were transferred from the air/water) all yielded light transmittance values that were higher than 85%.

The electrical conductance measurements in Figure 6B underscore the extraordinary long-range conductivities of the gold micro-wires. The current-voltage (*I–V*) curves depicted in Figure 6B were recorded through thermally evaporated gold electrodes upon the glass-supported micro-wire films at the inter-electrode spacings indicated in the graphs. Importantly, the linear *I–V* relationships apparent in all electrode distances indicate Ohmic behavior of electron transport.[30] Furthermore, the high current values observed for all electrode spacings (and corresponding sheet resistance of between around 20 Ω sq^{-1}) confirm that efficient electron transport occurred within the gold micro-wires over considerable distances, from hundreds of microns (Figure 6B) and up to several centimeters (Figure 6C and Figure S4).

The conductance measurements in Figure 6C further provide a dramatic manifestation that the direction of electron transport

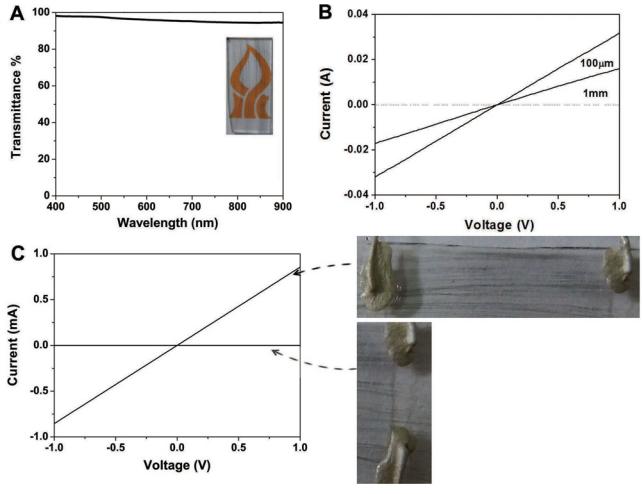

Figure 6. Optical transparency and electrical conductance of gold micro-wire films. (A) Transmittance spectrum. The inset shows a picture of the Au film deposited on glass and placed upon a text feature; (B) Current/voltage (I/V) curves recorded for thermally evaporated square electrodes at distances of 100 μm and 1 mm, respectively; (C) Current/voltage curves recorded for pasted silver electrodes parallel (top picture on the right), and vertical (bottom picture on the right) to the aligned Au micro-wires, respectively. Electrode distance was 2 cm.

depended upon the orientation of the gold micro-wires relative to the surface-pasted electrodes. Specifically, Figure 6C shows that electric current was recorded only when the two electrodes were placed in positions linked by parallel-oriented micro-wires; no current (e.g. flat *I–V* curve) was detected between two electrodes pasted in positions that were vertical to the micro-wire alignment. This result confirms that electron transport occurred only through the gold micro-wires, and demonstrates that macro-scale organization achieved by the new micro-wire fabrication technique provides the means for controlling the physical properties of the films generated.

3. Conclusions

In conclusion, we have developed a facile bottom-up method for fabricating extremely long, aligned, conductive gold micro-wires. The gold micro-wires were spontaneously formed through binding and subsequent crystallization/reduction of water-soluble $Au(SCN)_4^-$ upon a template of octyl-melamine monolayer. Transfer of the micro-wires onto solid substrates followed by plasma treatment/gold enhancement yielded highly transparent films exhibiting excellent conductivity up to electrode distances of several centimeters. Overall, the new scheme offers a simple, inexpensive, and robust platform for fabricating extremely long conductive gold micro-wires that can be employed in transparent conductive electrodes and other applications in electronics and photonics.

Experimental Section

Materials: $HAuCl_4 \cdot 3H_2O$, KSCN, 2-chloro-4,6-diamino-1,3,5-triazine, octadecylamine and anhydrous sodium hydrogencarbonate were purchased from Sigma-Aldrich and were used as received. The $Au(SCN)_4^-$ complex was prepared according to previous studies.[23] Briefly, 1 mL solution of $HAuCl_4 \cdot 3H_2O$ in water (24 mg mL^{-1}) was added to 1 mL solution of KSCN in water (60 mg mL^{-1}). The precipitate formed was separated by centrifugation at 4000 g for 10 min. The supernatant was decanted and the residue was dried at room temperature. The synthesis of OM molecule was carried out according to published procedures.[31,32] Briefly, a mixture of 2-chloro-4,6-diamino-1,3,5-triazine (19 mmol), octadecylamine (19 mmol) and anhydrous sodium hydrogencarbonate (19 mmol) in 1,4-dioxan (75 mL) was refluxed under argon atmosphere for 6 hrs. The reaction mixture was then cooled and poured into water (100 mL). The precipitation was filtered off and washed with water. The product was purified by flash chromatography on silicagel, eluting with a dichloromethane/methanol 10:1 mixture. Water used in the experiments was doubly purified using a Barnstead D7382 water purification system (Barnstead Thermolyne, Dubuque, IA), at 18.3 mΩ cm resistivity.

Octyl Melamine (OM) Monolayers: A computerized Langmuir trough (model 622/D1, Nima Technology Ltd., Coventry, UK) was used for isothermal compression of OM molecules. A solution of the OM in chloroform was prepared at a concentration of 1 mg mL^{-1}. Specific volumes of the solution were spread over pure water subphase or water containing $Au(SCN)_4^-$ in the Langmuir trough. After solvent evaporation, the barriers of the trough were compressed at a rate of 10 cm^2 min^{-1}. The surface-pressure/area isotherm was recorded and the compression was performed from 340 cm^2 to 80 cm^2. The aligned microwires were formed during the compression process.

Au Micro-Wires Formation: The appropriate amount of the OM solution was spread over $KAu(SCN)_4$ subphase (10^{-5} M) in the Langmuir trough. In this stage, the amine moieties of OM (which are

positively-charged in the pH conditions employed) and the negatively-charged $Au(SCN)_4^-$ were attracted to each other through electrostatic interactions. Following incubation for a few hours, gradual formation of the surface-deposited Au films occurred, without co-addition of external reducing agents – a common precondition in the large majority of gold metallization processes.[19,23,24] Indeed, different than almost all Au nanostructure reaction pathways, in this case the ligand (thiocyanate) is the reducing agent, likely according to Equation (1):

$$4H_2O + 2\mathrm{Au(III)}(SCN)_4^- \rightarrow 2AU(0) + SO_4^{2-} + CN^- + 8H^+ + 7SCN^- \quad (1)$$

After for 6 h, the barriers of the trough were compressed at a rate of 10 cm^2 min^{-1}. The surface-pressure/area isotherm was recorded and the compression was performed from 340 cm^2 to 80 cm^2. The aligned micro-wires were transferred onto hydrophobic silica wafer or glass substrates by the Langmuir-Schaefer (LS) method. After plasma treatment (Harrick Plasma PDC-32G, in High RF) for 3 min to remove the organic materials, the samples were ready for gold enhancement. Gold enhancement (seeding) was accomplished by dissolving $HAuCl_4$ (20 mg) in water (1 mL), which was added to a KSCN solution (1 mL, 60 mg mL^{-1}). The precipitate formed was separated from the solution using a centrifuge (4000 g) and added to a 8 mL of 1 M buffer solution of phosphoric acid (pH 5.5). A solution of hydroquinone (1 mL, 5.5 mg mL^{-1}), which constituted the reducing agent, was added to the buffer solution. The Au micro-wires transferred onto the solid substrate was then immersed for 3 min immediately after adding the hydroquinone. Subsequently, the substrate was gently washed with water. Note that when higher concentrations of $KAu(SCN)_4$ were used in the subphase we observed more pronounced deposition of gold, giving rise to enlarged Au domains rather than Au fibers.

Brewster Angle Microscopy (BAM): A Brewster angle microscope (NFT, Gottingen, Germany) mounted on a Langmuir film balance was used to observe the microscopic structures in situ at the air/water interface. The light source of the BAM was a frequency-doubled Nd:YAG laser with a wavelength of 532 nm and 20–70 mW primary output power in a collimated beam. The BAM images were recorded with a charge coupled device (CCD) camera. The scanner objective was a Nikon superlong working distance objective with a nominal 10× magnification and a diffraction-limited lateral resolution of 2 μm. The images were corrected to eliminate side ratio distortion originating from a non-perpendicular line of vision of the microscope.

Characterization: Scanning electron microscopy (SEM) images were recorded using a Jeol JSM-7400F Scanning electron microscope (JEOL LTD, Tokyo, Japan) at an acceleration voltage of 3 kV. Atomic force microscopy (AFM) images were recorded at ambient conditions in tapping mode using a Digital Instrument Dimension 3100 mounted on an active anti-vibration table. XPS analysis was carried out using Thermo Fisher ESCALAB 250 instrument with a basic pressure of 2×10^{-9} mbar. Powder x-ray diffraction (XRD) patterns were obtained using Panalytical Empyrean powder diffractometer equipped with a parabolic mirror on incident beam providing quasi-monochromatic Cu Kα radiation (λ = 1.54059 Å) and X'Celerator linear detector. UV-vis transparency measurements were carried out using a JASCO V-550 UV/vis spectrophotometer.

Conductivity Measurements: 100 μm square electrodes with spacings of 100 μm and 1 mm, respectively, composed of 10 nm Cr and 90 nm Au, were thermally evaporated on glass substrate. Prior to the thermal evaporation the samples were inserted to a plasma cleaner, PDC-32G, Harrick plasma, and were exposed to plasma for 3 min under vacuum. Room temperature conductivity measurements were carried out in a two-probe configuration using a probe station equipped with a Keithley 4200SCS semiconductor parameter analyzer.

Supporting Information

Supporting Information is available from the Wiley Online Library or from the author.

Acknowledgements

We are grateful for the Ministry of Science, Infrastructure Program, for financial support. Dr. Hao Jiang is grateful for PBC Program of Fellowships for Outstanding Post-doctoral Researchers from China and India.

Received: April 11, 2014
Revised: June 9, 2014
Published online: July 7, 2014

[1] Z. W. Pan, Z. R. Dai, Z. L. Wang, *Science* **2001**, *291*, 1947.
[2] L. Jiang, Y. Y. Fu, H. X. Li, W. P. Hu, *J. Am. Chem. Soc.* **2008**, *130*, 3937.
[3] A. Sugunan, P. Melin, J. Schnurer, J. G. Hilborn, J. Dutta, *Adv. Mater.* **2007**, *19*, 77.
[4] J. Y. Tang, Z. Y. Huo, S. Brittman, H. W. Gao, P. D. Yang, *Nat. Nanotechnol.* **2011**, *6*, 568.
[5] Y. G. Sun, D. Y. Khang, F. Hua, K. Hurley, R. G. Nuzzo, J. A. Rogers, *Adv. Funct. Mater.* **2005**, *15*, 30.
[6] Y. L. Wang, T. Y. Wang, P. M. Da, M. Xu, H. Wu, G. F. Zheng, *Adv. Mater.* **2013**, *25*, 5177.
[7] J. Yeon, Y. J. Lee, D. E. Yoo, K. J. Yoo, J. S. Kim, J. Lee, J. O. Lee, S. J. Choi, G. W. Yoon, D. W. Lee, G. S. Lee, H. C. Hwang, *Nano Lett.* **2013**, *13*, 3978.
[8] T. Thurn-Albrecht, J. Schotter, G. A. Kästle, N. Emley, T. Shibauchi, L. Krusin-Elbaum, K. Guarini, C. T. Black, M. T. Tuominen, T. P. Russell, *Science* **2000**, *290*, 2126.
[9] J. -Y. Lee, S. T. Connor, Y. Cui, P. Peumans, *Nano Lett.* **2008**, *8*, 689.
[10] A. Liscio, E. Orgiu, J. M. Mativetsky, V. Palermo, P. Samori, *Adv. Mater.* **2010**, *22*, 5018.
[11] S. Hoeppener, R. Maoz, S. R. Cohen, L. F. Chi, H. Fuchs, J. Sagiv, *Adv. Mater.* **2002**, *14*, 1036.
[12] X. D. Chen, S. Lenhert, M. Hirtz, N. Lu, H. Fuchs, L. F. Chi, *Acc. Chem. Res.* **2007**, *40*, 393.
[13] S. Yoshimoto, Y. Honda, O. Ito, K. Itaya, *J. Am. Chem. Soc.* **2008**, *130*, 1085.
[14] C. Yu, H. Nakshatri, J. Irudayaraj, *Nano lett.* **2007**, *7*, 2300.
[15] S. Liu, R. Maoz, J. Sagiv, *Nano Lett.* **2004**, *4*, 845.
[16] B. S. Flavel, J. Yu, A. V Ellis, J. S. Quinton, J. G. Shapter, *Nanotechnology* **2008**, *19*, 445301.
[17] E. Dujardin, C. Peet, G. Stubbs, J. N. Culver, S. Mann, *Nano Lett.* **2003**, *3*, 413.
[18] R. Volinsky, R. Jelinek, *Angew. Chem. Int. Edit.* **2009**, *48*, 4540.
[19] A. Morag, L. Philosof-Mazor, R. Volinsky, E. Mentovich, S. Richter, R. Jelinek, *Adv. Mater.* **2011**, *23*, 4327.
[20] Z. Nie, A. Petukhova, E. Kumacheva, *Nat. nanotechnol.* **2010**, *5*, 15.
[21] T. Thai, Y. Zheng, S. H. Ng, S. Mudie, M. Altissimo, U. Bach, *Angew. Chem. Int. Edit.* **2012**, *51*, 8732.
[22] C. R. Hansen, F. Westerlund, K. Moth-Poulsen, R. Ravindranath, S. Valiyaveettil, T. Bjørnholm, *Langmuir* **2008**, *24*, 3905.
[23] A. Morag, N. Froumin, D. Mogiliansky, V. Ezersky, E. Beilis, S. Richter, R. Jelinek, *Adv. Funct. Mater.* **2013**, *23*, 5663.
[24] A. Morag, V. Ezersky, N. Froumin, D. Mogiliansky, R. Jelinek, *Chem. Commun.* **2013**, *49*, 8552.
[25] T. P. Vinod, S. Zarzhitsky, A. Morag, L. Zeiri, Y. Levi-Kalisman, H. Rapaport, R. Jelinek, *Nanoscale* **2013**, *5*, 10487.
[26] S. Cho, D. H. Kim, B. S. Lee, J. Jung, W. R. Yu, S. H. Hong, S. Lee, *Sensors and Actuators B* **2012**, *162*, 300.
[27] S. Meltzer, R. Resch, B. E. Koel, M. E. Thompson, A. Madhukar, A. A. G. Requicha, P. Will, *Langmuir* **2001**, *17*, 1713.
[28] Y. B. Vysotsky, A. A. Shved, E. A. Belyaeva, E. V. Aksenenko, V. B. Fainerman, D. Vollhardt, R. Miller, *J. Phys. Chem. B* **2009**, *113*, 13235.

[29] X. Huang, C. Li, S. G Jiang, X. S. Wang, B. W. Zhang, M. H. Liu, *Journal of Colloid and Interface Science* **2005**, *285*, 680.
[30] K. Dawson, M. Baudequin, N. Sassiat, A. J. Quinn, A. O'Riordan, *Electrochimica Acta* **2013**, *101*, 169.
[31] J. Barberá, L. Puig, P. Romero, J. L. Serrano, T. Sierra, *J. Am. Chem. Soc.* **2006**, *128*, 4487.
[32] W. L. Hu, Y. K. Chen, H. Jiang, J. G. Li, G. Zou, Q. J. Zhang, D. G. Zhang, P. Wang, H. Ming, *Adv. Mater.* **2014**, *26*, 3136.